Preliminary Simulation on Spaceborne Sparse Array Millimeter Wave Radar for GMTI

Xueyan Kang · Yunhua Zhang

Abstract

Spaceborne sparse array radar for ground moving targets indication (GMTI) has outstanding advantage over full array radar for constructing ultra-large aperture. Rapid development of millimeter wave (MMW) technology make it possible for realizing MMW GMTI radar, which is much more sensitive to slow moving ground target. The paper presented the system model of a multi-carrier frequency sparse array MMW radar as well as preliminary simulation results, which showed future application of the system is very promising.

Key words: Ground Moving Targets Indication (GMTI), Millimeter Wave (MMW), Multi-Carrier-Frequency Mode, Spaceborne Sparse Array, Space Time Adaptive Processing (STAP).

Ⅰ. Introduction

Ground moving targets indication (GMTI) by using spaceborne sparse array radar has been proposed as an effective way to resolve the slow ground moving target detection problem in principle [1~4]. The outstanding advantage of sparse array is high spatial resolution, which is helpful for improving the capability of slow target indication, but the undersampling of sparse array will cause the blind-zone and angle-ambiguity problems of detection due to grating lobes. These problems can be mitigated by using multi-carrier-frequency technique [2~6]. Because of the high sensitivity to slow moving target with MMW radar, we proposed to construct spaceborne sparse array MMW radar for GMTI application. Although clutter is also more sensitive to more high frequency, the main-beam width of radar and the Doppler spread of main-beam clutter become narrower than that of lower frequency. Therefore, MMW is more helpful for clutter suppression and GMTI than lower frequency. We expect to obtain high performance by taking the advantages of MMW in GMTI.

In the following, Section 2 analyzes the system model for the MMW radar in the multi-carrier-frequency mode. Section 3 presents simulation results based on the model developed in section 2. The paper ends in section 4 after drawing some preliminary conclusions.

Ⅱ. The System Model

2-1 Sparse Array Radar

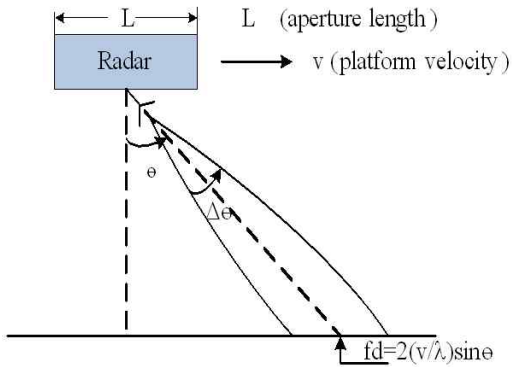

Fig. 1. The radar geometry.

For radar moving with velocity v, as shown in Fig. 1, the clutter return from the center of the beam will have a Doppler shift $f_d = 2(v/\lambda)\sin\theta$.

For an antenna of transverse length L and a beam of angular width $\Delta\theta = \lambda / L$, the main-beam clutter has a Doppler spread $\Delta f_d = (2v/L)\cos\theta$ about f_d. A target in the main beam, moving with ground velocity v_t, parallel to v, will similarly generate a Doppler frequency $f_{dt} = f_d + (2v_t/\lambda)\sin\theta$. To be detectable, the target Doppler has to be outside of the clutter-Doppler spread, Δf_d, leading to the condition $f_{dt} > \Delta f_d$.

At last, the minimum detectable velocity(MDV) of moving target is as follows:

$$MDV = (\frac{\lambda}{L}v)ctg\theta \quad (1)$$

The high platform velocity of spaceborne radar results

Manuscript received April 14, 2010 ; revised November 12, 2010. (ID No. 20100414-17J)
Center for Space Science and Applied Research, Chinese Academy of Sciences, Beijing, China.
Corresponding Author : Xueyan Kang (e-mail : kangxy@nmrs.ac.cn)

in a large main beam clutter spread, which limits the MDV of moving target. With typical values of v= 7,600 m/s and θ=45°, to obtain MDV=2 m/s, we need $L \geq$ 3,800 λ, which represents spaceborne GMTI radar need large aperture. However, it is impossible for a large filled aperture. Therefore it is a good solution using sparse array radar for spaceborne GMTI.

For the same MDV=2 m/s, the lengths of spaceborne sparse array need 836 m at the λ=0.22 m (L band), 114 m at the λ=0.03 m (X band) and 30 m at the λ=0.008 m(Ka band) from equation (1).

2-2 Synthetic Pattern of Sparse Linear Array

Let's assume a sparse linear array as [0, k_1, k_2,⋯,k_i, ⋯, k_{max-1}, k_{max}], in which the first aperture is a reference point that spatial sampling frequency is zero. Thus the actual position of the ith aperture can be calculated by $x_i = k_i \cdot B / k_{\max}$, where B is the longest baseline, k_i is the ith normalized spatial sampling frequency and $k_{\max}$ is the max normalized spatial sampling frequency.

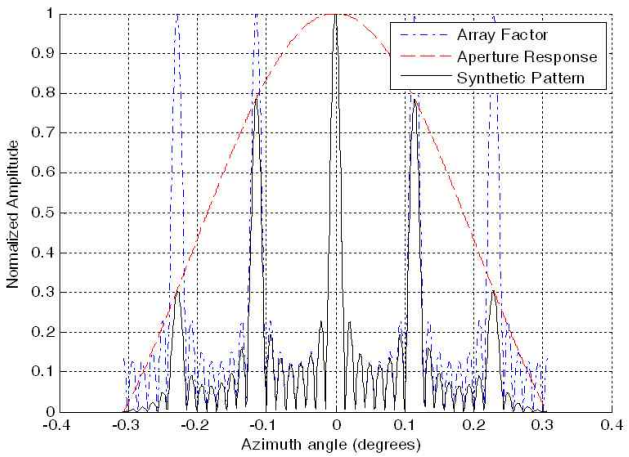

(a) ULA

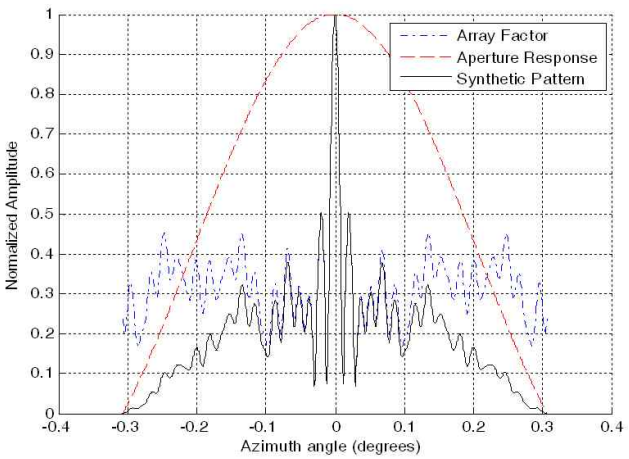

(b) MRA

Fig. 2. Construction of synthetic pattern for sparse linear array.

The synthetic pattern can be written as the product of array factor and aperture pattern: synthetic_pattern= array_factor*aperture_pattern [1]. We consider the following two configurations of sparse linear array in the paper (8 apertures as an example):

a) Uniform linear array (ULA): [0, 1, 2, 3, 4, 5, 6, 7]
b) Minimum redundancy array(MRA) : [0, 1, 4, 10, 16, 18, 21, 23]

For comparison, we set B=30 m, the center carrier frequency is 35 GHz.

Fig. 2 plot the synthetic pattern of ULA and MRA, The mainlobe of synthetic pattern becomes narrower than that of aperture pattern, which will decrease the minimum detectable velocity (MDV) of target and improve the GMTI performance. At the same time, we can see that there are many grating lobes due to undersampling of sparse array, which will cause angle ambiguities of target detection. Comparing (a) and (b), it is obvious that MRA reduces grating lobes, because the special layout of MRA will get the maximum spatial sampling frequency and minimum redundancy at the cost of the same elements and baseline.

Fig. 3 shows the grating lobe locations depend on transmitted frequency at the same element configuration, but the mainlobe location doesn't change with the different transmitted frequency. By integrating different signals transmitted at sufficiently different carrier frequencies, performance of target detection can be improved. So, the ambiguities of target can be mitigated by multi-carrier-frequency technique.

According to reference [8], spaceborne sparse array MMW radar can be designed on a single large satellite. Because of the advantage of MRA, MRA is adopted in the spaceborne sparse array MMW radar simulation.

2-3 STAP

Space time adaptive processing (STAP) combines spatial domain and temporal domain information to suppress the levels of the undesired interferers well below the small, desired signal returns [7]. STAP has proved to be one of the best techniques capable of detecting weak moving targets in strong clutter environment and has been widely applied in airborne GMTI radar. It is an effective method of clutter suppression in GMTI method.

2-4 System Model and Multi-Carrier-Frequency STAP

Fig. 4 briefly illustrates the working procedure of a multi-carrier-frequency radar system (the number of carrier fre-

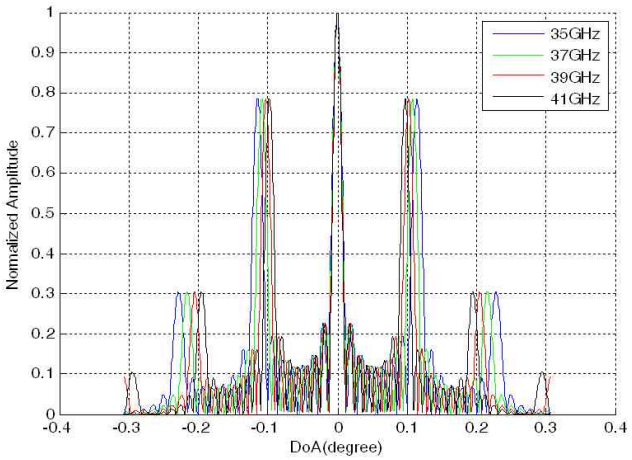

(a) ULA

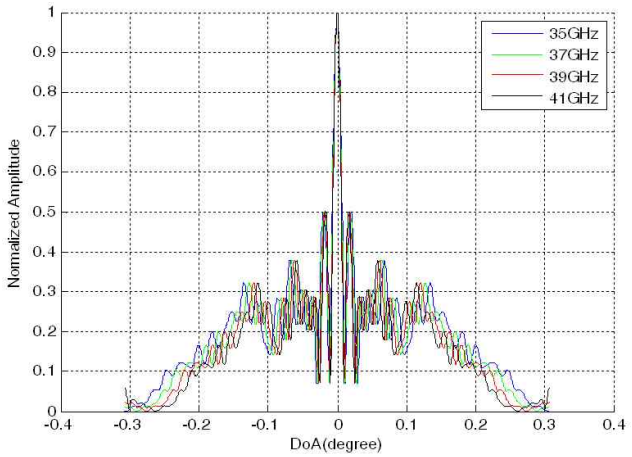

(b) MRA

Fig. 3. Effect of four different carrier frequencies(f_{c1}=35 GHz, f_{c2}=37 GHz, f_{c3}=39 GHz, f_{c4}=41 GHz).

quency K=3). In the multi-carrier-frequency system, band-pass filters(BPFs) are used to isolate signals from different band, at the same time each receiver can process K independent signal sets. We need design enough isolation of BPFs for system to avoid mutual coupling, which may affect antenna pattern and then decrease system performance.

Assume the number of carrier frequency is K ($K \leq N$), STAP processor receives a train of M pulses from each of N antenna elements with all K different frequencies collected over L range bins. So, we get the $K \times N \times M \times L$ data cube in multi-carrier-frequency STAP instead of the well known $N \times M \times L$ 3-D data cube in traditional STAP. The received data of the multi-carrier-frequency STAP system is described as Fig. 5. The principle of multi-carrier frequency STAP is as follows [3].

Consider the spaceborne sparse array radar as Fig. 6. In Fig. 6 we set $K = N$. We assume that one aperture transmits and all N apertures receive the reflected signal in a single-carrier-frequency mode. Each aperture trans-

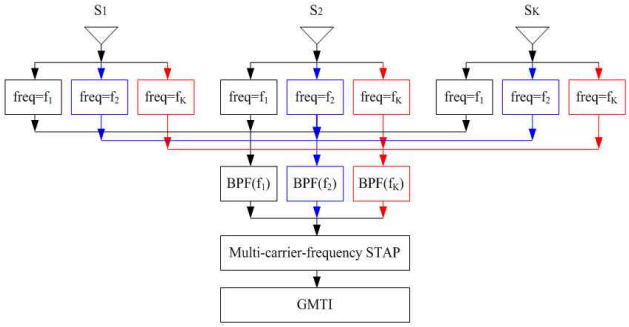

Fig. 4. Receiver structure of multi-carrier-frequency radar (The number of carrier frequency K=3).

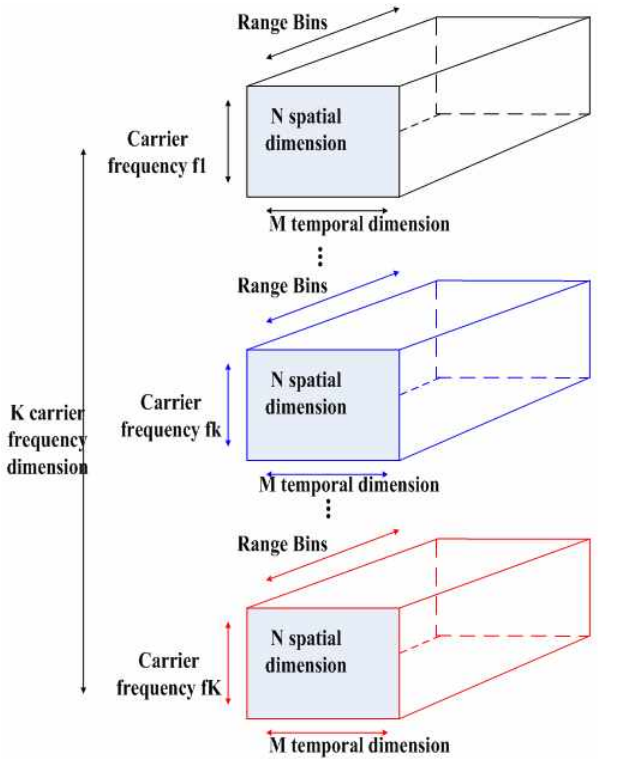

Fig. 5. Receiver data of multi-carrier-frequency STAP (The number of carrier frequency K=3).

mits signal, all N apertures receive the reflected signal transmitted by its own and other aperture transmitter in multi-carrier-frequency mode.

Assume the ith aperture transmit signals of the form:

$$S_{Ti}(t) = A_i(t)\exp(j2\pi f_{ci}t) \tag{2}$$

Where $A_i(t)$ is amplitude factor, for simplicity, we set $A_i(t)$=1, f_{ci} is the ith carrier frequency. Let $\{x_i\}$ denotes the positions of the N elements, each with corresponding carrier frequency $\{f_{ci}\}$, i=0, 1, 2,$\cdots$, $N-1$. Each aperture receives and processes the signals from all other N transmitters.

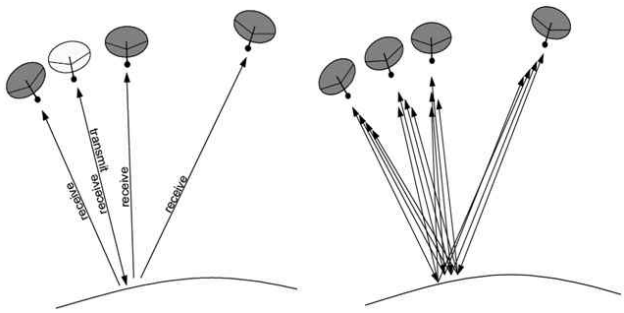

(a) Single-carrier frequency (b) Multi-carrier frequency

Fig. 6. Spaceborne radar for sparse linear array.

Consider each element transmits M pulses within a single coherent processing interval (CPI) at pulse repetition frequency of *prf*. We assume that *prf* is low enough to ignore range ambiguities, which may bring up Doppler ambiguities. Due to N transmissions, the return signal from a single target can be formed as a vector with length of N^2M. For a single target at the relative azimuth angle θ_p, at the kth carrier frequency f_k, space-time steering vector of length NM can be written as a Kronecker product of time steering vector $\mathbf{v}_t$ and space steering vector $\mathbf{v}_s$:

$$\mathbf{v}_k = \mathbf{v}_t \otimes \mathbf{v}_s \tag{3}$$

$$\mathbf{v}_t = \begin{bmatrix} 1 \\ \exp(j2\pi \frac{2vf_k}{c \cdot prf} \sin\theta_p) \\ \vdots \\ \exp(j2\pi(M-1)\frac{2vf_k}{c \cdot prf} \sin\theta_p) \end{bmatrix} \tag{4}$$

$$\mathbf{v}_s = \begin{bmatrix} 1 \\ \exp(j2\pi \frac{x_1 f_k}{c} \sin\theta_p) \\ \vdots \\ \exp(j2\pi \frac{x_{N-1} f_k}{c} \sin\theta_p) \end{bmatrix} \tag{5}$$

We assume that clutter in each range bin obeys Gaussian distribution independently, and the clutter signal for the kth carrier frequency f_k, space-time steering vector of length NM can be written as:

$$\mathbf{v}_{ck} = \zeta_k \mathbf{v}_{ct} \otimes \mathbf{v}_{cs} \tag{6}$$

where ζ_k is the amplitude of the clutter unit. The length N^2M space-frequency-time steering vector of clutter is

$$\mathbf{v}_c = [\mathbf{v}_{c0}^T \quad \mathbf{v}_{c1}^T \quad \cdots \quad \mathbf{v}_{ck}^T \quad \cdots \quad \mathbf{v}_{c(N-1)}^T]^T \tag{7}$$

Noise is modeled as a white complex Gaussian random variable for all frequencies, pulses and elements. The overall received signal, is therefore given by,

$$\mathbf{X}(l) = \alpha_t \mathbf{v}_t(v_t, \theta_t) + \mathbf{v}_c(l) + \mathbf{n} \tag{8}$$

where α_t is the amplitude of target, $\mathbf{v}_t(v_t, \theta_t)$ is target steering vector, and $\mathbf{n}$ is complex Gaussian noise vector. l denotes the lth range bin.

By using the signal in equation (8), we can implement a multi-frequency STAP algorithm. We select the optimal STAP where the N^2M elements of the received signal are processed using a weight vector

$$\mathbf{w}_{l/opt} = \mathbf{R}_l^{-1} \mathbf{v}_t \tag{9}$$

In equation (9) above, $\mathbf{R}_l$ is the clutter plus noise covariance matrix. In practice, $\mathbf{R}_l$ is unknown. We need to estimate it using equation (9).

$$\hat{\mathbf{R}}_l = \frac{1}{L} \sum_{m=1, m \neq l}^{L} \mathbf{X}_m \mathbf{X}_m^H \tag{10}$$

Thus the STAP output of the lth range bin in multi-carrier-frequency mode is

$$y_l = \mathbf{w}_l^H \mathbf{X}(l) = \sum_{i=1}^{N^2M} \mathbf{w}_l(i) \mathbf{X}_l(i) \tag{11}$$

In this analysis, to illustrate interference (clutter plus noise) suppression effect, SINR loss factor $L_{s,1}(\theta_P, f_d)$ is plotted as a function of azimuth angle [7].

$$L_{s,1}(\theta_P, f_d) = \frac{\sigma_s^2 \cdot |\mathbf{w}_l^H \mathbf{v}_t|^2 / \mathbf{w}_l^H \mathbf{R}_l \mathbf{w}_l}{MN^2 \cdot SNR_{element}} = \frac{\sigma_n^2 |\mathbf{w}_l^H \mathbf{v}_t|^2}{MN^2 \cdot (\mathbf{w}_l^H \mathbf{R}_l \mathbf{w}_l)} \tag{12}$$

where $\mathrm{SNR}_{\mathrm{element}}$ is the element signal-to noise ratio, σ_s^2 and σ_n^2 are power of signal and power of noise, respectively.

By using multiple different carrier frequencies, an additional diversity gain can be obtained on top of the advantages of spatial diversity. Therefore, these ambiguity problems can be mitigated through multi-carrier-frequency STAP.

In the following simulation, the numbers and the offset of carrier frequency are traded off in order to obtain the better performance and less computation.

Ⅲ. Simulation Results

Now we analyze the simulation results of optimal STAP for spaceborne sparse array MMW radar. Here we assume the system has eight apertures distributed along track and the longest baseline is B=30 m. The main parameters for radar system simulation are listed in Table 1. The system uses multi-carrier-frequency mo-

Table 1. Simulation parameters.

Parameters	Numerical value
Numbers of elements	8
Pulses in CPI	16
Center frequency	35 GHz
The number of carrier frequencies	4
The offset of carrier frequency	2 GHz
PRF	2,100 Hz
Subarray	1.5*1.5 m^2
H	800 km
Satellite platform velocity	7,435 m/s
CNR	30 dB
Target azimuth angle	−0.1°
Target velocity	2 m/s
Range bin of target	150
SNR	0 dB

des (In practice, the design of carrier frequency offset should consider many factors, such as the element numbers and configuration of sparse array, the number of carrier frequencies, antenna scanning scope, computation complexity, etc).

We study the two configurations of sparse linear array in the paper:

a) Uniform linear array (ULA): [0, 1, 2, 3, 4, 5, 6, 7], its actual positions of the 8 elements are [0, 4.2857, 8.5714, 12.8571, 17.1429, 21.4286, 25.7143, 30.0000] (m)

b) Minimum redundancy array (MRA): [0, 1, 4, 10, 16, 18, 21, 23], its actual positions of the 8 elements are [0, 1.2857, 5.1429, 12.8571, 20.5714, 23.1429, 27.0000, 30.0000] (m)

From Fig. 7(b), we can see the serious angle and Doppler ambiguities of target with the ULA configuration. Comparing Fig. 7 and Fig. 8 corresponding to the SINR loss and target detection results with two configurations, it is clear that MRA get a better result than ULA, because MRA meets the largest spatial sampling frequency and reduces the sparse degree at the same

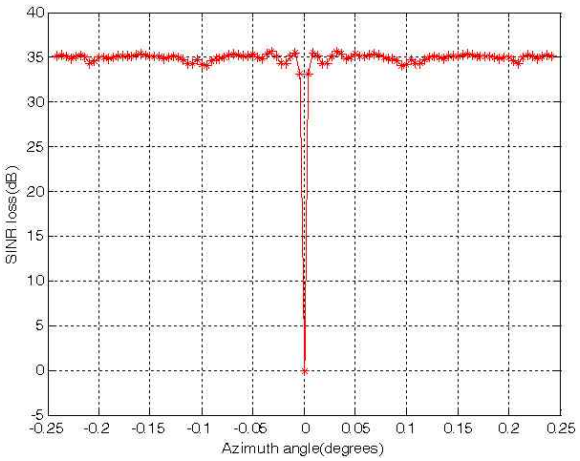

(a) SINR loss

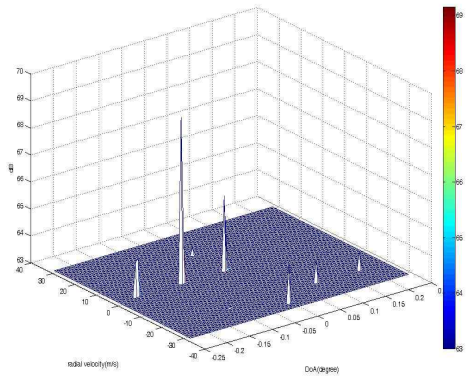

(b) Detection result of target after clutter suppression

Fig. 7. Multi-carrier-frequency STAP (ULA).

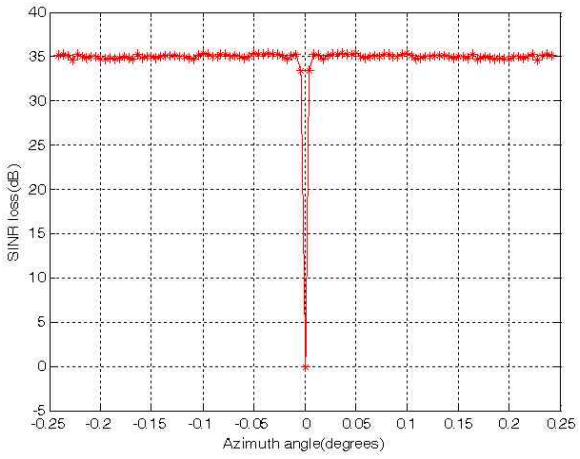

(a) SINR loss

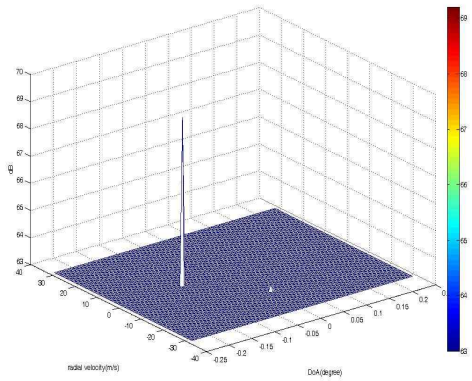

(b) Detection result of target after clutter suppression

Fig. 8. Multi-carrier-frequency STAP (MRA).

elements and baseline. Therefore, performance of MRA is better than ULA.

Ⅳ. Conclusion

The paper studied spaceborne sparse array radar working at millimeter wave (MMW) frequency for GMTI application. Based on the model of sparse linear array, the paper firstly simulated synthetic pattern of ULA and MRA, and then analyzed the system model and optimal STAP for spaceborne sparse array with multi-carrier-frequency mode. At the same time, MRA was considered to mitigate the ambiguity problems. Finally, the paper presented preliminary simulations to show that spaceborne sparse array MMW radar with MRA configuration for GMTI has a promising future.

Comparing with centimeter wave radar, MMW radar had the advantage of high angular resolution, wide bandwidth, large Doppler shift and small antenna in physical dimensions, but its disadvantage is relatively severer atmospheric absorption, therefore, MMW radar usually needs larger transmission power. It is expected that with the development of MMW technology, much high efficiency MMW device would be available in the future to obtain larger output power with lower cost, which can help to solve this problem.

References

[1] K. Marais, R. Sedwick, "Space based GMTI using scanned pattern interferometric radar(SPIR)," *IEEE International Radar Conference*, USA: Atlanta, Georgia, pp. 2047-2055, 2001.

[2] D. A. Leatherwood, W. L. Melvin, and R. Acree, "Configuring a sparse aperture antenna for spaceborne MTI radar," *IEEE International Radar Conference*, pp. 139-146, 2003.

[3] R. Adve, R. Schneible, and R. McMillan, "Adaptive space/frequency processing for distributed aperture radars," *IEEE International Radar Conference*, pp. 160-164. 2003.

[4] R. S. Adve, R. A. Schneible, G. Genello, and P. Antonik, "Waveform-space-time adaptive processing for distributed aperture radars," *IEEE International Radar Conference*, pp. 93-97, May 2005.

[5] E. Lock, R. S. Adve, "Orthogonal frequency division multiplexing in distributed radar apertures," *IEEE International Radar Conference*, pp. 488-493, 2008.

[6] L. Zhuang, X. Liu, "Application of frequency diversity to suppress grating lobes in coherent MIMO radar with separated subapertures," *EURASIP Journal on Advances in Signal Processing*, 2009. hin dawi.com

[7] W. L. Melvin, "A STAP overview," *IEEE Trans. on AES*, vol. 19, no. 1, pp.19-35, 2004.

[8] M. A. Fischman, C. Le, and P. A. Rosen, "A digital beamforming processor for the joint DoD/NASA space based radar mission," *IEEE Radar Conference*, pp. 9-14, 2004.

Xueyan Kang

received the B.S. and M.S. degrees in electronics and information system from Northwest University, Xi'an, China in 1998 and 2001, and the Ph.D. degree in communication and information system from Institute of electronics, Chinese Academy of Sciences, in 2004. She is now an associate researcher with the Center for Space Science and Applied Research, Chinese Academy of Sciences. Her main research interests are radar signal processing.

Yunhua Zhang

received the B.S. degree from Xi-dian University, Xi'an, China, and the M.S. and Ph.D. degrees from Zhejiang University, Hangzhou, China, in 1989, 1993 and 1995, respectively, all in electrical engineering. He is now a professor with the Center for Space Science and Applied Research, Chinese Academy of Sciences. His research interests cover the system design and signal processing of microwave sensors, as well as computational electromagnetics.